

Kris Hauser

Indiana University
Lindley Hall, Room 215,
Bloomington,
IN 47405-7104, USA
hauserk@indiana.edu

Jean-Claude Latombe

Stanford University
Clark Center, Room S244
Stanford,
CA 94305, USA
latombe@cs.stanford.edu

Multi-modal Motion Planning in Non-expansive Spaces

Abstract

Motion planning problems encountered in manipulation and legged locomotion have a distinctive multi-modal structure, where the space of feasible configurations consists of intersecting submanifolds, often of different dimensionalities. Such a feasible space does not possess expansiveness, a property that characterizes whether planning queries can be solved efficiently with traditional probabilistic roadmap (PRM) planners. In this paper we present a new PRM-based multi-modal planning algorithm for problems where the number of intersecting manifolds is finite. We also analyze the completeness properties of this algorithm. More specifically, we show that the algorithm converges quickly when each submanifold is individually expansive and establish a bound on the expected running time in that case. We also present an incremental variant of the algorithm that has the same convergence properties, but works better for problems with a large number of submanifolds by considering subsets of submanifolds likely to contain a solution path. These algorithms are demonstrated in geometric examples and in a legged locomotion planner.

KEY WORDS—motion planning, probabilistic completeness, hybrid systems, legged locomotion

1. Introduction

Probabilistic roadmap (PRM) planners (Choset et al. 2005, Chapter 7) are state-of-the-art approaches for motion plan-

ning in high-dimensional configuration spaces under geometrically complex feasibility constraints. They approximate the connectivity of the robot's feasible space \mathcal{F} by a network of configurations sampled according to suitable probabilistic measures and connected by simple paths. It is well known that PRMs can be slow when \mathcal{F} has poor *expansiveness* (Hsu et al. 1997) or, informally, contains “narrow passages” (Hsu et al. 1998). In non-expansive spaces where \mathcal{F} consists of intersecting submanifolds of varying dimensionality, submanifolds of lower dimensionalities form arbitrarily thin passages, and PRM planners do not work at all.

This type of *multi-modal* structure happens in motion planning problems found in manipulation, legged locomotion, and reconfigurable robots. Here, each submanifold in \mathcal{F} corresponds to a *mode*, a fixed set of contact points maintained between the robot and its environment (or between locations on the robot itself). The planner must choose a discrete sequence of modes (hence, a sequence of contacts to make and break), as well as continuous single-mode paths through them (the joint space motions to achieve those changes of contacts).

In problems where each mode defines a low-dimensional submanifold, such as planar manipulation of multiple objects (Alami et al. 1995; Nieuwenhuisen et al. 2006; Stilman 2007; van den Berg et al. 2008), the primary challenge lies in the combinatorial complexity of mode sequencing. However, in problems with high-dimensional submanifolds, the complexity of single-mode planning poses an additional challenge. Complete single-mode planning is intractable, so PRM planners are often used for such planning. This approach has made it possible to solve several specific problems in both manipulation with grasps and regrasps (Koga and Latombe 1994; Nielsen and Kavraki 2000; Sahbani et al. 2002) and legged locomotion (Bretl et al. 2004); (Hauser et al. 2006). However,

a PRM planner cannot report that no path exists, so when a single-mode query fails, we cannot tell whether the query is truly infeasible or the planner just needed more time. So, in general, the overall reliability of the multi-modal planner may degrade substantially, as it often makes tens of thousands (or more) of single-mode queries to the PRM planner. So far, little attention has been paid to the theoretical performance guarantees of these algorithms when applied to general multi-modal problems.

In this paper we present `Multi-Modal-PRM`, a general-purpose multi-modal planning algorithm for problems with a finite number of modes, and investigate its theoretical completeness properties. `Multi-Modal-PRM` builds a PRM across modes by sampling configurations in \mathcal{F} and in the transitions between modes (the intersections of the corresponding submanifolds). We prove that if each mode is favorably expansive when restricted to its embedded submanifold, then like classical PRM planners, `Multi-Modal-PRM` will eventually find a feasible path if one exists, and convergence is fast. The convergence rate is exponential, which allows us to establish that expected running time is finite, as is the variance in running time.

We also present a more practical variant, `Incremental-MMPRM`, which searches for a small candidate subset of modes which are likely to contain a solution path, and then restricts `Multi-Modal-PRM` to these modes. `Incremental-MMPRM` has the same asymptotic completeness properties as `Multi-Modal-PRM`, but is usually much faster for problems with a large number of modes (a common situation in practice). We present experiments that illustrate the sensitivity of our algorithms to the number of modes, the number of mode switches needed to reach the goal, and expansiveness of each mode relative to its embedded submanifold. We also demonstrate the application of `Incremental-MMPRM` in the legged locomotion planner of Hauser et al. (2006), showing that it is indeed reliable.

Section 2 describes how PRM planners can be used to solve multi-modal planning problems. Section 3 presents the `Multi-Modal-PRM` algorithm and gives an overview of its completeness properties. Section 4 proves that `Multi-Modal-PRM` is probabilistically complete and exponentially convergent, and also derives upper bounds on the mean and variance of its running time. Section 5 describes the more practical `Incremental-MMPRM` algorithm. Section 6 describes some variants in the sampling strategy that further improve practical performance. Section 7 reports on experimental results obtained with our algorithms. Finally, Section 8 concludes the paper and discusses future work, including the case where there is a continuous infinity of modes.

2. Multi-modal Planning

This section defines multi-modal planning problems, describes how PRM planners can be used to solve these problems,

and outlines the pitfalls that make many existing PRM-based multi-modal planners incomplete.

2.1. PRM Planners and Non-expansive Spaces

PRM planners approximate the connectivity of \mathcal{F} , the feasible subset of a robot's configuration space, using a roadmap of configurations (referred to as *milestones*) connected by simple paths (usually straight lines) (Kavraki et al. 1996). The concept of expansiveness was introduced to characterize how quickly a roadmap converges to an accurate representation (Hsu et al. 1997, 1999). In the Appendix, we briefly review the basic PRM algorithm and its convergence properties in expansive spaces.

The expansiveness of \mathcal{F} is measured by three parameters ϵ , α , and β (see the Appendix) that all take values in $[0, 1]$. These values only depend on the relative volumes of certain subsets of \mathcal{F} , and not on its dimensionality. If all three parameters have positive values, then \mathcal{F} is expansive; otherwise it is non-expansive. In all expansive spaces, the probability that the basic PRM planner given in the Appendix fails to solve a planning query decreases to zero exponentially as the roadmap grows. The larger ϵ , α , and β , the quicker the convergence. Conversely, convergence can become arbitrarily slow as ϵ , α , or β approaches zero. Poorly expansive spaces (i.e. spaces where ϵ , α , and β are low) contain narrow passages. Fortunately, smoothed analysis shows that narrow passages are unstable with respect to small perturbations of the input geometry, and are therefore unlikely to occur (except by design) (Chaudhuri and Koltun 2007). In other words, poorly expansive spaces are rare in practice.

However, some non-expansive spaces do exist, not by chance, but rather for structural reasons. If \mathcal{F} contains a cusp (then $\epsilon = 0$), it is non-expansive, but PRMs might still work well everywhere away from the cusp, since removing tiny regions around the cusp makes \mathcal{F} expansive without changing its connectivity (Kavraki et al. 1998). If \mathcal{F} contains regions of varying dimensionality (then α or $\beta = 0$), it is also non-expansive. For example, this is the case of the space \mathcal{F} shown in Figure 1, which consists of two two-dimensional regions (\mathcal{F}_1 and \mathcal{F}_2) connected by a one-dimensional curve (\mathcal{F}_3). In this space, the "narrow" passage formed by \mathcal{F}_3 has null relative volume and a PRM planner is unable to find a path connecting the two-dimensional regions, even after an arbitrary amount of time.

Varying dimensionality is *inherent* in the structure of multi-modal problems. In these problems, if the number of modes is finite, the submanifolds whose union forms \mathcal{F} can be enumerated from the problem definition, e.g. by considering all possible combinations of contacts. However, their number may be enormous.

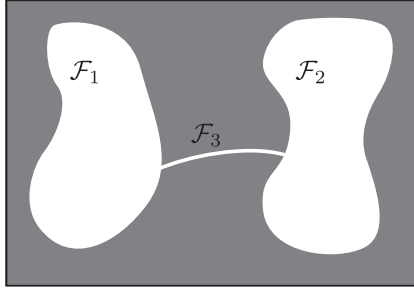


Fig. 1. A non-expansive, multi-modal feasible space \mathcal{F} can be decomposed into three modes that are individually expansive.

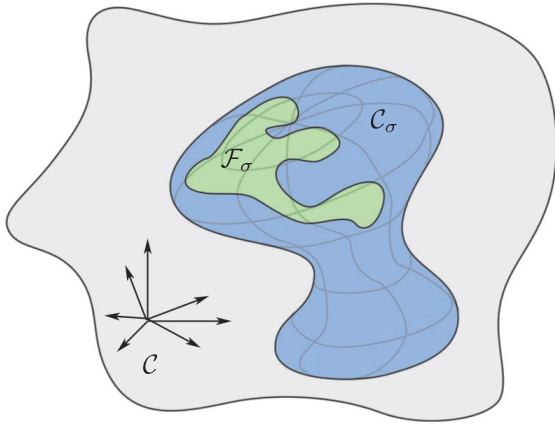


Fig. 2. At a mode σ , motion is constrained to a subset \mathcal{F}_σ of a submanifold \mathcal{C}_σ with lower dimension than \mathcal{C} .

2.2. Multi-modal Problem Definition

Consider a robot that can move between a *finite* set Σ of modes (in the conclusion of this paper, we briefly discuss the case where there is a continuous infinity of modes). A specific feasible space \mathcal{F}_σ corresponds to each mode $\sigma \in \Sigma$, and $\mathcal{F} = \bigcup_{\sigma \in \Sigma} \mathcal{F}_\sigma$ (Figure 1). The feasibility constraints of a mode can be divided into two classes.

- *Dimensionality-reducing* constraints, often represented as functional equalities $C_\sigma(q) = 0$. They define the submanifold \mathcal{C}_σ as the set of configurations that satisfy these constraints.
- *Volume-reducing* constraints, often represented as inequalities $D_\sigma(q) > 0$. These may cause \mathcal{F}_σ to be empty. Otherwise, \mathcal{F}_σ has the same dimension as \mathcal{C}_σ but smaller volume (Figure 2).

For example, in legged locomotion, σ is defined by a fixed set of footfalls. Here \mathcal{F} can be embedded in a configuration

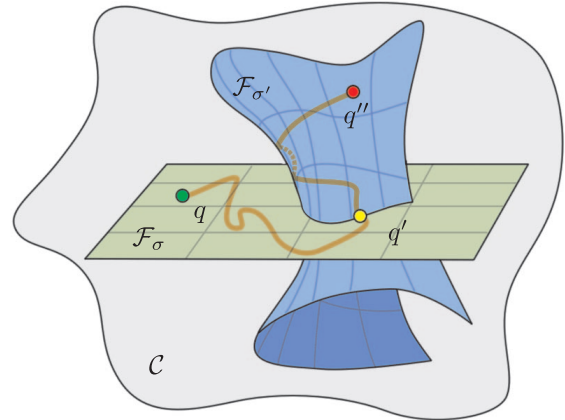


Fig. 3. To move from configuration q at stance σ to q'' at an adjacent stance σ' , the motion must pass through a transition configuration q' .

space \mathcal{C} , which consists of parameters for a free-floating robot base and the robot's joint angles. Enforcing contact at the footfalls imposes kinematic constraints, which in turn define \mathcal{C}_σ (a submanifold of uniform lower dimension, except at singularities). Collision avoidance and static stability constraints are volume-reducing, and restrict \mathcal{F}_σ to a subset of \mathcal{C}_σ .

2.3. Planning Between Two Modes

PRMs planners can be used for single-mode planning restricted to \mathcal{C}_σ . When \mathcal{C}_σ is not a linear space (e.g. there are closed-loop kinematic chains), this requires adapting configuration sampling and path generation between milestones. Two approaches are parameterizing \mathcal{C}_σ with an atlas of charts (Cortés and Siméon 2004) and using numerical methods to move configurations from the ambient space onto \mathcal{C}_σ (LaValle et al. 1999). A PRM planner will plan quickly as long as \mathcal{F}_σ (with \mathcal{C}_σ as the ambient space) is expansive.

Let the robot be at configuration q in mode σ . To switch to a new mode σ' , it must plan a path in \mathcal{F}_σ that ends in a configuration q' in $\mathcal{F}_\sigma \cap \mathcal{F}_{\sigma'}$ (Figure 3). The region $\mathcal{F}_\sigma \cap \mathcal{F}_{\sigma'}$ is called the *transition* between σ and σ' , and q' is called a *transition configuration*. Transitions are at least as constrained as σ or σ' because they must simultaneously satisfy the constraints of both stances. Hence, for most pairs σ, σ' , they are empty. When they are not empty, they often have zero volume relative to \mathcal{C}_σ or $\mathcal{C}_{\sigma'}$. Thus, transition configurations should be sampled explicitly from $\mathcal{C}_\sigma \cap \mathcal{C}_{\sigma'}$. Like single-mode sampling, transition sampling can be performed using explicit parameterization or numerical techniques (Hauser et al. 2005a).

The existence of a configuration q' is a necessary condition for a single-mode path to connect q and σ' , and is a good indication that a feasible path exists (since there are fewer constraints in single-mode spaces). Sampling a configuration q'

from the region $\mathcal{F}_\sigma \cap \mathcal{F}_{\sigma'}$ is also typically much faster than planning a single-mode path in \mathcal{F}_σ that ends in $\mathcal{F}_\sigma \cap \mathcal{F}_{\sigma'}$. These two observations are instrumental in the implementation of Incremental-MMPRM (Section 5). However, the existence of q' is not sufficient for a path to exist, because q and q' might lie in different connected components of \mathcal{F}_σ .

2.4. Planning in Multiple Modes

Because PRM planners usually work well for single-mode planning, multi-modal planning is usually addressed by computing several single-mode plans and concatenating them into a multi-modal plan. Given a finite set of modes $\{\sigma_1, \dots, \sigma_m\}$, a multi-modal planner explores a *mode graph* \mathcal{G} where each vertex represents a mode and an edge connects every pair of *adjacent* modes. This assumes that there exists a computationally cheap adjacency test that checks a necessary condition for the existence of a path moving between two given modes σ and σ' . For example, an adjacency test in legged locomotion tests whether σ' adds exactly one footfall within the reach of σ (i.e. makes a new potentially reachable contact), or retracts one footfall from σ (i.e. breaks one contact). This test is very fast, but nevertheless prunes out many unnecessary edges from \mathcal{G} .

Because \mathcal{G} tends to be extremely large, one natural strategy explores only a small part of \mathcal{G} . For example, a search-like algorithm incrementally builds a tree \mathcal{T} of configurations reachable from the start configuration of the robot. Each expansion step picks a configuration q in \mathcal{T} . Then for every mode σ' adjacent to the mode σ of q , it queries a PRM planner to compute a feasible single-mode path from q to a transition configuration q' in $\mathcal{F}_\sigma \cap \mathcal{F}_{\sigma'}$. If the outcome is successful, q' is added to \mathcal{T} . These steps are repeated until the goal is reached.

2.5. Completeness Challenges in Multi-modal Planning

Special challenges arise when combining several single-mode PRM queries to solve a multi-modal problem. Multi-Modal-PRM addresses the following issues, any of which may cause a planner to fail to find a path.

Because any single-mode query might be infeasible (in practice, a large fraction of them are actually infeasible), the PRM planner must be terminated with failure after some cutoff time. Set the cutoff too low, and the planner may miss critical paths; set it too high, and the planner wastes time on infeasible queries. Some prior work tries to avoid infeasible queries (Koga and Latombe 1994; Bretl et al. 2004; Hauser et al. 2005a), allowing the cutoff to be set high. Another approach avoids cutoffs by interleaving computation among queries (Nielsen and Kavraki 2000; Hauser et al. 2005a; Nieuwenhuisen et al. 2006).

Because transitions $\mathcal{F}_\sigma \cap \mathcal{F}_{\sigma'}$ may have zero volume in \mathcal{F}_σ or $\mathcal{F}_{\sigma'}$, transition configurations should be sampled explicitly

from $\mathcal{C}_\sigma \cap \mathcal{C}_{\sigma'}$. Furthermore, more than one configuration q' may need to be sampled in each transition $\mathcal{F}_\sigma \cap \mathcal{F}_{\sigma'}$, because a configuration may lie in a component that is disconnected in \mathcal{F} from the start configuration, or one that is disconnected in \mathcal{F}' from a target configuration.

3. Multi-Modal-PRM

This section presents the general Multi-Modal-PRM algorithm, and gives an overview of its theoretical completeness properties. These properties will be proven in the following section.

3.1. Algorithm

Multi-Modal-PRM builds PRMs across all modes, connecting them at explicitly sampled transition configurations (see Figure 4 for an illustration). Suppose that there are m modes, so $\Sigma = \{\sigma_1, \dots, \sigma_m\}$. For each $\sigma_i \in \Sigma$ the algorithm maintains a roadmap \mathcal{R}_{σ_i} of \mathcal{F}_{σ_i} . Let the sampler `Sample-Mode`(σ_i) be defined as follows. Uniformly sample a configuration q at random from \mathcal{C}_{σ_i} . If q is in \mathcal{F}_{σ_i} , `Sample-Mode` returns q ; if not, it returns failure. Let us define `Sample-Trans`(σ_i, σ_j) similarly to rejection sample from $\mathcal{F}_{\sigma_i} \cap \mathcal{F}_{\sigma_j}$. Multi-Modal-PRM is given q_{start} and q_{goal} , the start and goal configurations of the robot, and an iteration limit N . The algorithm is defined as in Algorithm 1.

Algorithm 1 Multi-Modal-PRM($q_{\text{start}}, q_{\text{goal}}, N$)

Add q_{start} and q_{goal} as milestones to the roadmaps corresponding to their modes (σ_{start} and σ_{goal}).

Repeat N times:

1. For each mode σ_i , sample a configuration q using `Sample-Mode`(σ_i). If it succeeds, add q to \mathcal{R}_{σ_i} as a new milestone, and connect it to existing milestones in \mathcal{R}_{σ_i} .
2. For each pair of adjacent modes σ_i and σ_j , sample a configuration q using `Sample-Trans`(σ_i, σ_j). If it succeeds, add q to \mathcal{R}_{σ_i} and \mathcal{R}_{σ_j} , and connect it to milestones in \mathcal{R}_{σ_i} and \mathcal{R}_{σ_j} .

Build an aggregate roadmap \mathcal{R} by connecting roadmaps at matching transition configurations.

If q_{start} and q_{goal} are connected by a path in \mathcal{R} , terminate with success. Otherwise, return failure.

The running time of N iterations of Multi-Modal-PRM is dominated by roadmap construction, which can be computed as follows. Assume that configuration sampling and feasibility checking each take $O(1)$ time, and let D be the maximum

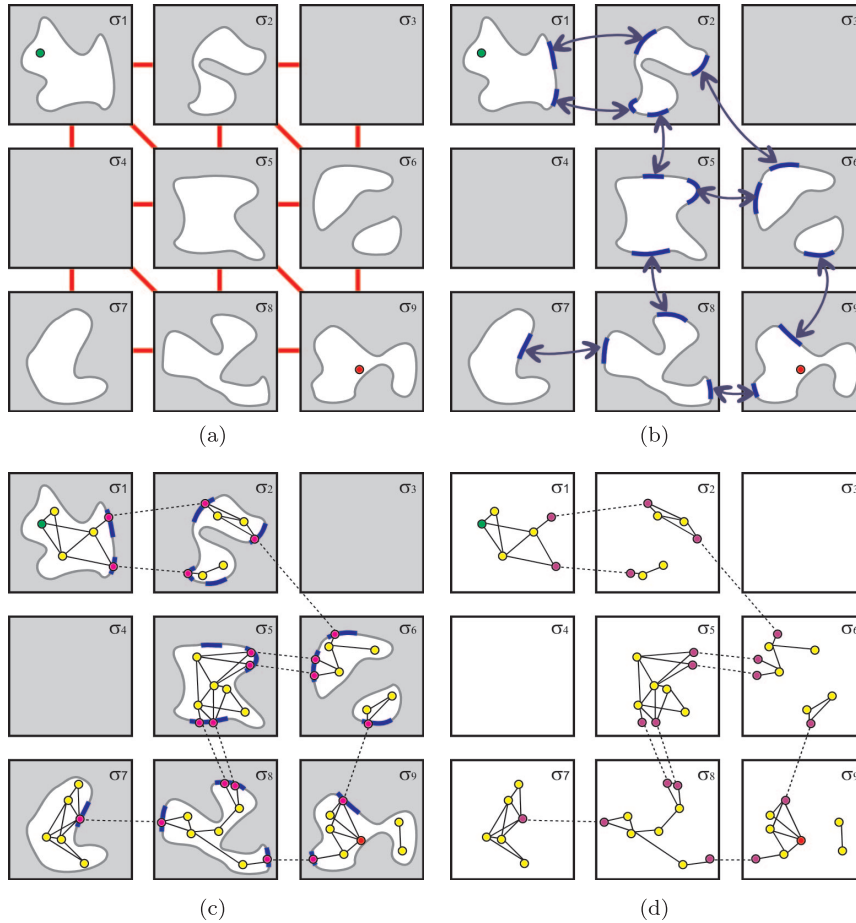


Fig. 4. Illustrating Multi-Modal-PRM on an abstract example problem. (a) A mode graph with nine modes, with adjacent modes connected by lines. (b) The transition regions, with arrows indicating how they map between modes. A path that switches from one mode to an adjacent mode must pass through a transition region, but it is not known *a priori* whether the region is non-empty. (c) Building roadmaps, using milestones sampled from modes (light dots) and milestones sampled from transitions (dark dots). Dashed lines connect two transition configurations that are identical, but are included as milestones in different modes. (d) The aggregate roadmap.

number of adjacencies of any mode. After N iterations, each single-mode roadmap may contain at most N milestones sampled from the mode and ND milestones sampled from transitions, so each roadmap requires checking $O(N^2D^2)$ edges for collision. Since there are m modes, the total running time is $O(mD^2N^2)$, or $O(DN^2|\mathcal{G}|)$.

3.2. Summary of Theoretical Results

Section 4 will prove that, under certain conditions, the probability that Multi-Modal-PRM incorrectly returns failure when a feasible path actually exists is less than ce^{-dN} , where c and d are positive constants and N is the number of iterations. This means that as more time is spent planning, the probability of failure decreases quickly to zero. The constants c and d

do not explicitly depend on the number m of modes or the dimensionalities of the spaces \mathcal{F}_{σ_i} , $i = 1, \dots, m$. Furthermore, since a constant number of samples ($|\mathcal{G}|$) are drawn per iteration, Multi-Modal-PRM also converges exponentially in the total number of samples drawn.

This bound holds if the following conditions are met:

1. The set of modes $\Sigma = \{\sigma_1, \dots, \sigma_m\}$ is finite.
2. If \mathcal{F}_{σ_i} is non-empty, then it is expansive.
3. If \mathcal{F}_{σ_i} is non-empty, $\text{Sample-Mode}(\sigma_i)$ succeeds with non-zero probability.
4. If $\mathcal{F}_{\sigma_i} \cap \mathcal{F}_{\sigma_j}$ is non-empty, $\text{Sample-Trans}(\sigma_i, \sigma_j)$ samples each connected component of $\mathcal{F}_{\sigma_i} \cap \mathcal{F}_{\sigma_j}$ with non-zero probability.

Suppose that Multi-Modal-PRM is implemented such that it iterates until a solution path is found. Section 4.5 shows that under the above conditions, the expected number of iterations needed is bounded by

$$E[N] \leq \frac{\log c}{d} + \frac{1}{1 - e^{-d}}. \quad (1)$$

Likewise, we show the variance of N is bounded by a function of c and d .

4. Proof of Completeness Properties

This section proves that Multi-Modal-PRM is probabilistically complete and exponentially convergent in the number of iterations. The proof shows that three processes exponentially converge: (1) Basic-PRM under rejection sampling; (2) roadmaps connecting transition components; and (3) roadmaps along any sequence of modes which contains a feasible multi-step path. We also prove finite bounds on average running time and variance in running time.

4.1. Exponential Convergence

Let $\bar{X}(N)$ denote the event that a process X fails after N iterations. We say that process X (and event $\bar{X}(N)$) is *exponentially convergent* in N if $Pr(\bar{X}(N)) \leq ae^{-bN}$, where a and b are positive constants. A useful *composition principle* allows us to avoid stating the coefficients a and b , which become cumbersome. If two quantities are subject to exponentially decreasing upper bounds, their sums and products are themselves subject to exponentially decreasing bounds. The product is trivial, and $a_1e^{-b_1N} + a_2e^{-b_2N}$ is upper bounded by ae^{-bN} for $a = (a_1 + a_2)$ and $b = \min b_1, b_2$. So, if two independent events $\bar{X}(N)$ and $\bar{Y}(N)$ are exponentially convergent in \bar{N} , then $\bar{Z}(N) = \bar{X}(N) \wedge \bar{Y}(N)$ or $\bar{Z}(N) = \bar{X}(N) \vee \bar{Y}(N)$ are also exponentially convergent in N .

4.2. Convergence of Basic PRM Planning in a Single-mode Feasible Space

The basic PRM planning algorithm given in the Appendix was proven by Hsu et al. (1997) to converge exponentially in the number of milestones. Our first lemma is a minor extension, and states that PRM planning also converges exponentially in the number of rejection samples drawn.

Let p be the probability that a random sample from \mathcal{C} lies in \mathcal{F} . This probability is non-zero whenever \mathcal{F} has non-zero volume in \mathcal{C} . From N configurations uniformly sampled at random from \mathcal{C} , let the milestones \mathcal{M} be those that are feasible.

Lemma 1. *If \mathcal{F} is expansive and $p > 0$, the probability that a roadmap \mathcal{R} constructed from \mathcal{M} connects two query configurations q_1 and q_2 converges to 1 exponentially in N .*

Proof. Since the configuration samples are independent, the size of \mathcal{M} is binomially distributed. The inequality of Hoeffding (1996) gives an upper bound to the probability that \mathcal{M} has n or fewer milestones:

$$Pr(|\mathcal{M}| \leq n) \leq \exp(-2(Np - n)^2/N).$$

If $|\mathcal{M}| \leq n$, the probability of failure is at most 1. On the other hand, if $|\mathcal{M}| > n$, the probability that \mathcal{R} fails to connect q_1 and q_2 is less than ce^{-dn} , where c and d are the constants in Theorem 2 (see the Appendix). Since these events are mutually exclusive, the overall probability of failure ν is bounded as follows:

$$\begin{aligned} \nu &\leq Pr(|\mathcal{M}| \leq n) \cdot 1 + Pr(|\mathcal{M}| > n)c \exp(-dn) \\ &\leq \exp(-Np^2/2) + c \exp(-Ndp/2), \end{aligned} \quad (2)$$

where we have set $n = pN/2$. Using the composition principle, this bound is exponentially decreasing in N . \square

4.3. Convergence of Connecting Transition Components

Here we consider the probability of finding a path in $\mathcal{F} = \mathcal{F}_\sigma$ between two transition components A and B , by building a roadmap using N rejection samples in each of the three set A , B , and \mathcal{F} . Here A and B may be components of two distinct transitions $\mathcal{F}_\sigma \cap \mathcal{F}_{\sigma'}$ and $\mathcal{F}_\sigma \cap \mathcal{F}_{\sigma''}$, or two distinct components of the transition $\mathcal{F}_\sigma \cap \mathcal{F}_{\sigma'}$. (Indeed, a path may have to make a detour through \mathcal{F}_σ to connect two components of $\mathcal{F}_{\sigma'}$.)

Let \mathcal{M} and p be defined as in Lemma 1. Let us rejection sample A and B , respectively, by drawing samples uniformly at random from supersets A' and B' , with probability of success p_A and p_B . Again, p_A (respectively p_B) are non-zero whenever A' (B') has non-zero volume in A (B). From N configurations sampled from A' , let \mathcal{M}_A be the set of milestones in A . Define \mathcal{M}_B similarly.

Lemma 2. *Assume that \mathcal{F} is expansive, and p , p_A , and p_B are non-zero. Let \mathcal{R} be the roadmap constructed from all milestones \mathcal{M} , \mathcal{M}_A , and \mathcal{M}_B . If A and B are in the same connected component of \mathcal{F} , then the probability that \mathcal{R} contains a path between A and B converges to 1 exponentially in N .*

Proof. View any pair of milestones q_A in \mathcal{M}_A and q_B in \mathcal{M}_B as PRM query configurations. Then \mathcal{R} contains a path between A and B when \mathcal{M}_A is non-empty (event X), \mathcal{M}_B is non-empty (event Y), and the roadmap formed from \mathcal{M} connects q_A and q_B (event Z).

The probability that N rejection samples from A' fails to find a milestone in A is at most $(1 - p_A)^N \leq e^{-Np_A}$. So, event X is exponentially convergent in N . The same holds for Y . Finally, event Z is exponentially convergent in N by Lemma 1 and since q_A and q_B are in the same connected component. The lemma holds by applying the composition principle to X , Y , and Z . \square

4.4. Convergence of Multi-Modal-PRM

Lemma 3. *Let the assumptions at the end of Section 3 hold. Between any two configurations, if any feasible multi-step path exists, there exists some feasible path that makes a finite number of mode switches.*

Proof. Expansiveness of a feasible space \mathcal{F} implies that every connected component of \mathcal{F} has volume at least $\epsilon > 0$ (see Appendix A.2). Let ϵ be such that every connected component of each single-mode feasible space \mathcal{F}_{σ_i} , $i = 1, \dots, m$, has volume at least $\epsilon > 0$. Then, each space \mathcal{F}_{σ_i} contains at most $1/\epsilon$ components and the overall feasible space contains at most m/ϵ components.

If there exists a feasible multi-modal path between two configurations and if this path visits more than once the same connected component of a single-mode feasible space \mathcal{F}_{σ_i} , then this path can be “shortened” into a new path that visits \mathcal{F}_{σ_i} only once. Therefore, there exists a feasible path that visits each component of each single-mode feasible space at most once. This path makes a finite number of mode switches. \square

Theorem 1. *Let the assumptions at the end of Section 3 hold. If q_s and q_g can be connected with a feasible multi-step path, then the probability that Multi-Modal-PRM finds a path converges to 1 exponentially in the number of iterations N .*

Proof. If q_s and q_g can be connected with a feasible path, there is a feasible path with a finite number of mode switches. Suppose that this path travels through mode σ_k , $k \in \{1, \dots, m\}$, from transition component A to transition component B . Sample-Mode and Sample-Trans have properties allowing Lemma 2 to be applied to roadmap \mathcal{R}_{σ_k} . Therefore, the probability that \mathcal{R}_{σ_k} connects A and B exponentially converges to 1. The theorem follows from repeating this argument for all modes along the path, and using the composition principle a finite number of times. \square

The number of modes m and the dimensionalities of the spaces \mathcal{F}_{σ_i} do not explicitly affect the coefficients in the convergence bound (although the total cost per iteration is at least linear in m). On the other hand, Multi-Modal-PRM converges more quickly when both the expansiveness of the single-mode feasible spaces and the parameters p and p' increase. Convergence is also quicker if fewer modes are needed

to reach the goal or if the goal can be reached via multiple paths.

4.5. Expected Running Time

Consider an implementation of Multi-Modal-PRM that continues iterating until a solution path is found. The algorithm is probabilistically complete, because it will find a path with probability 1 as long as a solution exists. However, this condition alone is insufficient to guarantee that average running time is bounded. For example, if the probability of failure within N iterations is $1/N$, then expected running time is infinite. Because Multi-Modal-PRM is exponentially convergent, we can show that the number of iterations needed to find a solution has finite expected value and variance.

We bound the expected running time of Multi-Modal-PRM by considering worst-case behavior. Let the random variable N_w denote the iteration on which Multi-Modal-PRM terminates under the assumption of worst-case behavior. Then, the bound on the probability of failure e^{-dN} is tight, and $\max\{0, 1 - ce^{-dN}\}$ describes the cumulative distribution function (CDF) of N_w . Since ce^{-dN} is greater or equal to 1 when $N \leq \log c/d$, the probability that $N_w \leq \log c/d$ is zero. For simplicity of the remaining argument, assume that $\log c/d$ is integer-valued. Once N exceeds $\log c/d$, the bound decreases according to a geometric distribution, i.e. a coin flip. So, the random variable X defined as $N_w - \log c/d$ has a geometric distribution with CDF e^{-dX} , and its expected value is $E[X] = 1/(1 - e^{-d})$. Therefore, the expected number of iterations is bounded by

$$E[N] \leq E[N_w] = \log c/d + 1/(1 - e^{-d}), \quad (3)$$

which is finite. Since each iteration takes bounded time, the expected running time is finite.

To bound the variance in running time, we use the fact that $\text{Var}(N) = E[N^2] - E[N]^2 \leq E[N^2] \leq E[N_w^2]$. Letting $N_0 = \log c/d$, we expand as follows:

$$\begin{aligned} E[N_w^2] &= \sum_{N=N_0+1}^{\infty} N^2 e^{-d(N-N_0)} = \sum_{N=1}^{\infty} (N + N_0)^2 e^{-dN} \\ &= \sum_{N=1}^{\infty} (N^2 + 2NN_0 + N_0^2) e^{-dN} \\ &= \sum_{N=1}^{\infty} N^2 e^{-dN} + 2N_0 \sum_{N=1}^{\infty} N e^{-dN} \\ &\quad + N_0^2 \sum_{N=1}^{\infty} e^{-dN}. \end{aligned} \quad (4)$$

The first summation in (4) is equal to $E[X^2]$, which can be computed as

$$E[X^2] = \text{Var}(X) + E[X]^2 = \frac{e^{-d}}{(1 - e^{-d})^2} + \frac{1}{(1 - e^{-d})^2}. \quad (5)$$

The second summation in (4) is equal to $E[X] = 1/(1 - e^{-d})$, and the third is equal to 1. Replacing these values in (4) and after some additional manipulation, we find the following bound on the variance $\text{Var}(N)$:

$$\text{Var}(N) \leq \frac{e^{-d}}{(1 - e^{-d})^2} + \left(\frac{1}{1 - e^{-d}} + \frac{\log c}{d} \right)^2. \quad (6)$$

5. An Incremental Variant

Incremental-MMPRM

Even executing a few iterations of Multi-Modal-PRM is impractical if the number of modes is large. In our experiments, legged locomotion problems frequently involve over a billion modes, while only tens or hundreds of steps are needed to go anywhere within the range of visual sensing. The Incremental-MMPRM variant uses heuristics to produce a small subset of modes that are likely to contain a path to the goal. Limiting planning to these modes make planning much faster. However, heuristics are not always right, so Incremental-MMPRM is designed to gracefully degrade back to Multi-Modal-PRM if necessary.

5.1. Overview

Incremental-MMPRM alternates between *expansion* and *refinement* steps. At each round $r = 1, 2, \dots$, it restricts itself to building roadmaps over a candidate set of modes Σ_r . It sets Σ_0 to the empty set, and all single-mode roadmaps (except those containing the start and goal configurations) are initially empty. The algorithm repeats the following steps for round $r = 1, \dots, Q$:

1. *Expansion.* Add new modes to Σ_{r-1} to produce the next candidate mode set Σ_r . If Σ_r contains all modes, proceed according to Multi-Modal-PRM.
2. *Refinement.* Incrementally build roadmaps in Σ_r . Specifically, draw N_{old} samples for each mode and transition in Σ_{r-1} , and draw N_{new} mode and transition samples for each new mode and transition in Σ_r . Add feasible samples to the appropriate roadmaps in Σ_r as in Multi-Modal-PRM.

We set N_{new} much higher than N_{old} , because sampling has a higher chance of improving roadmap connectivity in poorly sampled modes than in heavily sampled modes. Choosing the

value of these parameters involves some trade-offs, which are discussed in more detail in Section 6.

The performance of Incremental-MMPRM depends mainly on the expansion heuristics that are used to select the new candidate modes. These heuristics do not affect asymptotic convergence, as long as the candidate mode set grows until it cannot expand any further (at which point Incremental-MMPRM behaves exactly like Multi-Modal-PRM). However, in practice, they have a major impact on running time. The method presented below can be applied to any multi-modal planning problem. Our tests show that it improves running time by orders of magnitude.

5.2. Expansion: Search Among Feasible Transitions

In virtually all multi-modal problems we have studied, one may consider a huge number of modes and transitions, but *most* of them are actually infeasible, i.e. have empty feasible spaces. Trying to sample such spaces would cause the planner to waste a considerable amount of time. Instead, if the expansion step produces candidate modes that are likely to contain a feasible path, overall planning speed will be improved, even if expansion incurs some additional computational expense.

Search among feasible transitions (SAFT) uses the existence of a feasible transition between two modes σ and σ' as a good indication that a feasible path also exists between a configuration in \mathcal{F}_σ and a configuration in $\mathcal{F}_{\sigma'}$ (similarly to Bretl et al. (2004)). Indeed, as mentioned in Section 2.3, all of the constraints imposed by both σ and σ' apply at the transition, which can be seen as the bottleneck between \mathcal{F}_σ and $\mathcal{F}_{\sigma'}$. (This assumption may not hold in some pathological cases; in Section 7.2 we construct an example that violates this assumption, and Incremental-MMPRM performs poorly.)

So, SAFT incrementally builds the mode graph \mathcal{G} (starting from the mode σ_{start} of the start configuration), but without expanding an edge until it has sampled a feasible transition configuration. To avoid missing transitions with low volume, SAFT interleaves transition sampling between modes (as in Hauser et al. (2005a)). It maintains a list \mathcal{A} of “active” transitions. Each transition T in \mathcal{A} has an associated priority $p(T)$, which decreases as more time has been spent sampling T . The SAFT algorithm is given as Algorithm 2.

The steps of the algorithm are illustrated in Figure 5.

5.3. Mode Ordering Heuristics

The choice of priority function $p(T)$ is a design decision that strongly affects the behavior of SAFT. It is certain that $p(T)$ should decrease as more samples are drawn on T to avoid perpetually sampling a single infeasible transition T . It is not clear what other information it should encode, and a good choice may be carefully tailored to the problem. Some reasonable examples are as follows:

Algorithm 2 Search Among Feasible Transitions (SAFT)

SAFT-Init (performed only once before round 1)

Add the start mode σ_{start} to \mathcal{G} . Initialize \mathcal{A} to contain all transitions to modes adjacent to σ_{start} . (Recall from Section 2.4 that adjacency is defined by a computationally cheap test that checks a necessary condition for the existence of a path between two given modes.)

SAFT-Expand(r) (used on expansion round r)

Repeat the following:

1. Remove a transition T from \mathcal{A} with maximum priority. Suppose that T is a transition from σ to σ' . Try to sample a configuration in $\mathcal{F}_\sigma \cap \mathcal{F}_{\sigma'}$.
2. On failure, reduce the priority $p(T)$ and reinsert T into \mathcal{A} .
3. On success, add σ' to the mode graph \mathcal{G} . For each transitions T' from σ' to a mode adjacent to σ' , add T' to \mathcal{A} with initial priority $p(T')$.

Repeat until \mathcal{G} contains a sequence of modes (not already existing in Σ_{r-1}) connecting σ_{start} to σ_{goal} (the mode of the goal configuration). Add the modes in this sequence to Σ_{r-1} to produce Σ_r .

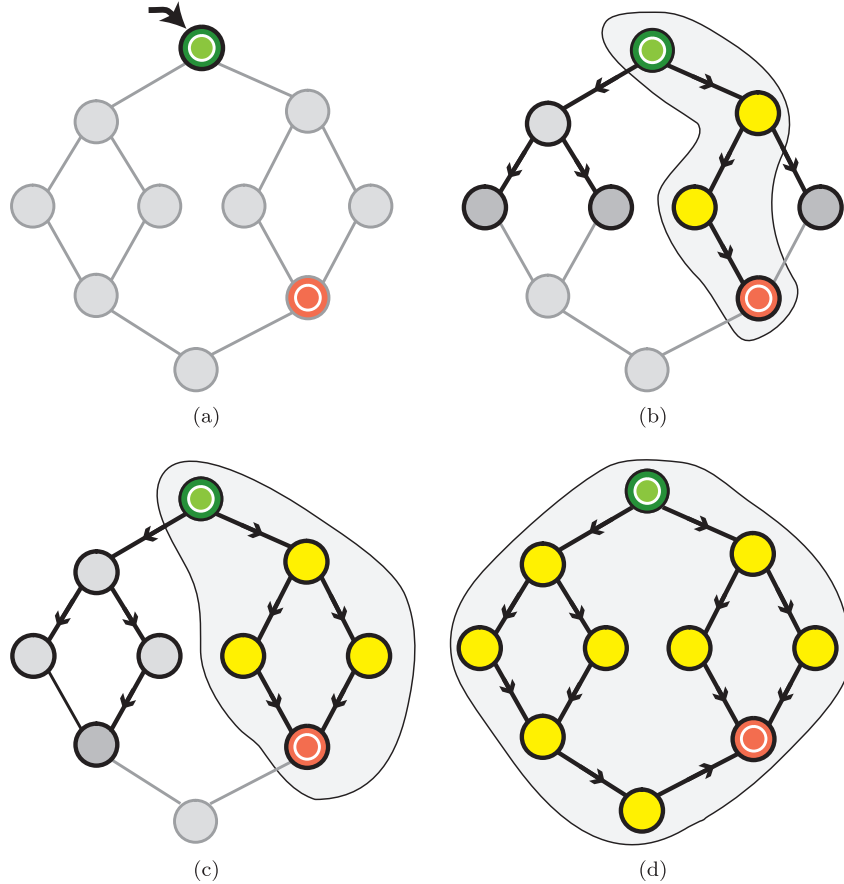


Fig. 5. Illustrating SAFT on a small mode graph. (a) The mode graph, with the start and goal mode marked with inset circles. (b) Search runs until the goal is reached. Nodes in the active set are darkened. The modes in the path leading to the goal (circled) are used as candidate modes for the refinement step. (c) If no feasible path is found, search continues until another route to the goal is found. The new mode is added to the candidate mode set. (d) If the candidate mode set becomes maximal, the algorithm proceeds like Multi-Modal-PRM.

- An uninformed choice is $p(T) = -n(T)$, where $n(T)$ is the number of samples drawn on T . With this choice, SAFT samples transitions that are recently added to the search tree more heavily. A similar approach was used by Nielsen and Kavraki (2000).
- The choice $p(T) = -g(T) - \alpha n(T)$ makes SAFT behave like breadth-first search, where $g(T)$ is the number of modes needed to reach T from the start mode, and α is a positive user-defined constant. As α grows, SAFT behaves more similarly to the uninformed case. As α shrinks toward 0, SAFT samples transitions that are shallow in the search tree more heavily.
- If we possess a heuristic $h(T)$ that estimates the number of modes needed to reach the goal, the choice $p(T) = -h(T) - g(T) - \alpha n(T)$ make SAFT explore more heavily closer to the goal (similar to A* search).
- A decision-theoretic approach, as taken by Hauser et al. (2005a), chooses $p(T)$ to estimate the probability that T is non-empty. In preprocessing, they learn a statistical model of the prior probability that the transition between two modes is non-empty, as a function of features of the modes. As more samples are drawn, $p(T)$ is adjusted to reflect the posterior probability.
- Other work has incorporated heuristics into $p(T)$ so that the planner favors modes that yield natural postures, are robust to disturbances, or are energy efficient (Hauser et al. 2006).

In the experiments of Section 7, we use the breadth-first search-like strategy (the second function described above).

6. Sampling Distributions and Single-mode Planning Strategies

This section suggests a number of ways to improve the running time of Multi-Modal-PRM and Incremental-MMPRM by tuning the distribution of samples among modes and transitions, and within modes.

6.1. Parameters Affecting Distribution Among Transitions and Modes

It is typically suboptimal to sample modes and transitions at a one-to-one ratio, because it often takes many more samples to plan paths in a mode than to sample the connected components of a transition. We control this ratio using a parameter $r_{M/T}$, which should be large if modes are expected to be poorly expansive, or transitions are likely to have a small number of connected components. Also, in Incremental-MMPRM, we

control the number of samples drawn during refinement steps by selecting parameters N_{new} and N_{old} . If too many samples are drawn, the planner might waste time on a candidate mode set that contains no feasible path; too few, and the planner may not find a path in the candidate mode set even when one exists, and it will continue to expand the candidate set unnecessarily. In practice, $r_{M/T}$, N_{new} , and N_{old} can be tuned manually to give good performance. For most parameter values (apart from 0 and ∞), the algorithms will still be exponentially complete, although with different convergence constants.

6.2. Belief-based Sampling

The above sampling distribution has two drawbacks. First, it does not prescribe a method to pick optimal parameters for a given problem, even if the structure of its feasible space is understood. Second, it samples modes evenly, which leads to wasting samples on “easy” (favorably expansive) modes or putting too few samples in “hard” (poorly expansive) modes. Difficulty is not known *a priori*, but can be inferred from information gathered during planning. For example, if a mode’s roadmap is already highly connected, then more samples are unlikely to improve connectivity. To address these issues, we use a belief-based sampling policy that adaptively estimates and transition difficulty, and picks a mode or transition sample to achieve the highest probability of improving roadmap connectivity.

The policy assumes the start and goal lie in the same connected component \mathcal{F}' . Consider a transition T between modes σ and σ' . We wish to estimate the probability $z(T)$ that the next sample in T will be the first feasible configuration in $\mathcal{F}' \cap \mathcal{F}_\sigma \cap \mathcal{F}_{\sigma'}$. Let $f(T)$ be the probability that we draw a feasible transition sample, and let $g(T)$ be the fraction of $\mathcal{F}_\sigma \cap \mathcal{F}_{\sigma'}$ that is in \mathcal{F}' . Assume that it is constant, so we drop the dependence on T . Then, if $m(T)$ feasible transition configurations have already been found, then we have $z(T) = f(T)g(1 - g)^{m(T)}$.

Now consider a mode σ . We wish to estimate the probability $z(\sigma)$ that the next sample added to \mathcal{R}_σ connects two configurations q and q' that are in distinct transitions out of σ and are also in \mathcal{F}' . Let $f(\sigma)$ be the probability of connecting two arbitrary configurations on the next sample. Let \mathcal{T}_σ be the set of transition configurations in \mathcal{R}_σ .

Suppose that we know that a subset S of the configurations in \mathcal{T}_σ lie in \mathcal{F}' . Then if \mathcal{R}_σ does not already connect two configurations in S that are in distinct transitions, the probability that the next sample added to the roadmap connects two transitions in S is

$$Pr(\text{Connect} \mid S) = 1 - (1 - f(\sigma))^{Pairs(S)},$$

where $Pairs(S)$ counts the number of potential connections in S . Here we have assumed that connections are independent,

which gains computational tractability at the expense of accuracy. If \mathcal{R}_σ already connects two transitions in S , we say $Pr(\text{Connect} \mid S) = 0$.

If a transition q in \mathcal{T}_σ is already connected to the start or goal, it must be in S . Otherwise, we do not observe whether q belongs to S , and instead we treat its membership probabilistically. We then marginalize $Pr(\text{Connect} \mid S)$ over all possible subsets S of \mathcal{T}_σ :

$$z(\sigma) = \sum_{S \subseteq \mathcal{T}_\sigma} Pr(\text{Connect} \mid S) g^{|S|} (1-g)^{|\mathcal{T}_\sigma| - |S|}. \quad (7)$$

The beliefs g , $f(T)$, and $f(\sigma)$ are estimated using data gathered in a preprocessing step. We use a set of training problem instances that are assumed to be similar to the testing problems, and build large roadmaps using Multi-Modal-PRM. The beliefs are computed as follows:

- For all transitions reachable from the start, we compute the fraction of transition configurations reachable from the start. We set g to this fraction.
- For each feasible transition, we compute the probability of drawing a feasible transition configuration, and fit these probabilities to a Beta prior. We compute $f(T)$ as the posterior when $N(T)$ samples have been drawn on T , and $m(T)$ are feasible.
- We construct the cumulative single-mode PRM success distribution $F(N)$ that measures the probability that two milestones are connected after N samples have been drawn. We assume that $F(N)$ is the same for all modes. We then let $f(\sigma)$ be the conditional function $F(N+1) - F(N) / (1 - F(N))$, where $N \equiv N(\sigma)$ is the number of samples previously drawn from σ .

6.3. Variants of the Single-mode Planner

Single-mode planning may be sped up using variants of Basic-PRM with more sophisticated sampling strategies. For example, the Gaussian sampling strategy (Boor et al. 1999) attempts to place more samples near the boundary of free space, and is typically faster than Basic-PRM on problems with narrow passages. Tree-growing planners, such as EST (Hsu et al. Mar 2002), RRT (LaValle and Kuffner, Jr. 2001), and SBL (Sánchez and Latombe 2002), are often faster when the task is to connect only two configurations. When considering multiple paths between all transition configurations in a mode, a tree-based planner can be adapted to the probabilistic roadmap-of-trees (PRT) approach (Akinc et al. 2003). In the legged locomotion experiments below, we use PRT with SBL as the underlying tree-based planner. In practice, we find that this approach is several times faster than Basic-PRM. It should be cautioned that, *a priori*, it is difficult to tell whether

a PRM variant will improve running time of the multi-modal planner. They may also affect convergence, because not all variants possess the same exponential convergence properties as Basic-PRM.

7. Experiments

Our first set of experiments compare Multi-Modal-PRM and Incremental-MMPRM in artificial, highly controlled, geometric configuration spaces. To summarize, the results match closely with the theoretical predictions: Multi-Modal-PRM is linearly dependent on the number of modes and slightly affected by goal depth, while Incremental-MMPRM is much more affected by goal depth than the number of modes. Both algorithms perform worse as the expansiveness of each mode decreases. We also investigate the effects of parameters N_{new} and N_{old} on the performance of Incremental-MMPRM.

In a second set of experiments, we apply the algorithms to a legged locomotion planner. We show that Multi-Modal-PRM consistently finds paths where a prior algorithm does not. We also evaluate the hypothesis that the performance improvements are due to Multi-Modal-PRM properly handling modes with disconnected feasible spaces.

7.1. Geometric Example A

Example A is depicted in Figure 6. The point robot moves in three dimensions, but is restricted to move in two-dimensional faces of cubes forming a $k \times k$ grid. Each cube provides four faces to the configuration space (the other two faces are not part of that space), and each face contains two rectangular obstacles that form a narrow passage. The total number of modes $m = 2k^2 + 2k$ is quadratic in k . Transitions are allowed along cube edges, so each mode is adjacent to at most six other modes. The passage has width w and length $1/3$, and expansiveness is controlled by varying w . Since the space is fully connected, any sequence of modes leading to the goal contains a solution. The goal is chosen such that the goal mode is at depth d in the search tree. These experiments use parameters $r_{M/T} = 10$, $N_{\text{new}} = 1,000$, $N_{\text{old}} = 0$ and the breadth-first-like priority function $p(T) = -g(T) - n(T)$.

Figure 7(a) shows that the running time of Multi-Modal-PRM is linearly dependent on the number of modes, while that of Incremental-MMPRM stays roughly constant. Figure 7(b) shows that the running time of Multi-Modal-PRM is not strongly affected by d , while Incremental-MMPRM slows as d increases. Figure 7(c) shows that running time for both algorithms improves as w (and thus single-mode expansiveness) grows.

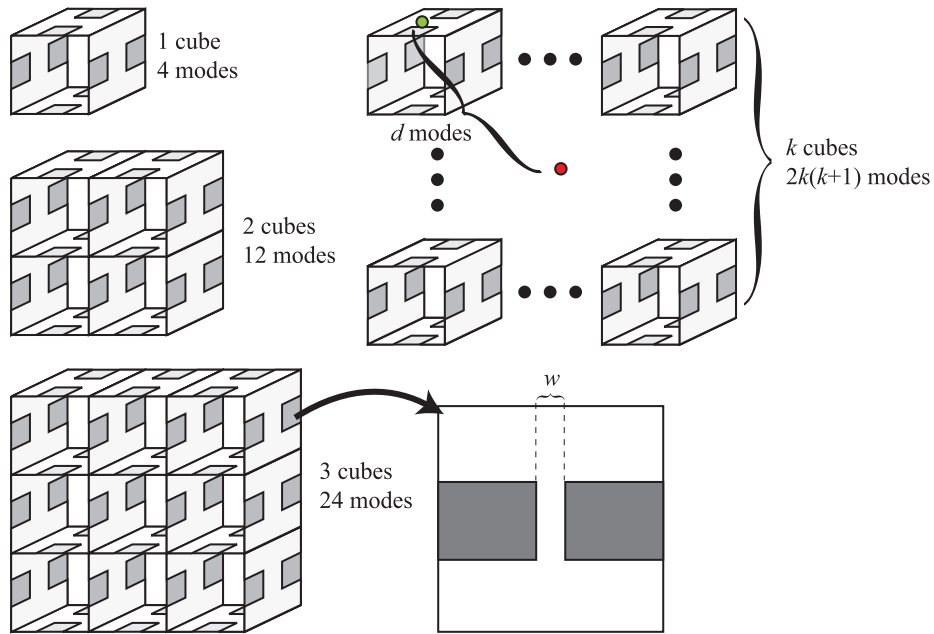


Fig. 6. In Example A, the point is restricted to move along the faces of cubes embedded in a three-dimensional space. Each mode has configuration space obstacles that form a narrow passage, illustrated on the right. The parameters are as follows: k is the number of cubes along each side; d is the depth of the goal mode; w is the width of the passage, and thus controls the expansiveness of each mode.

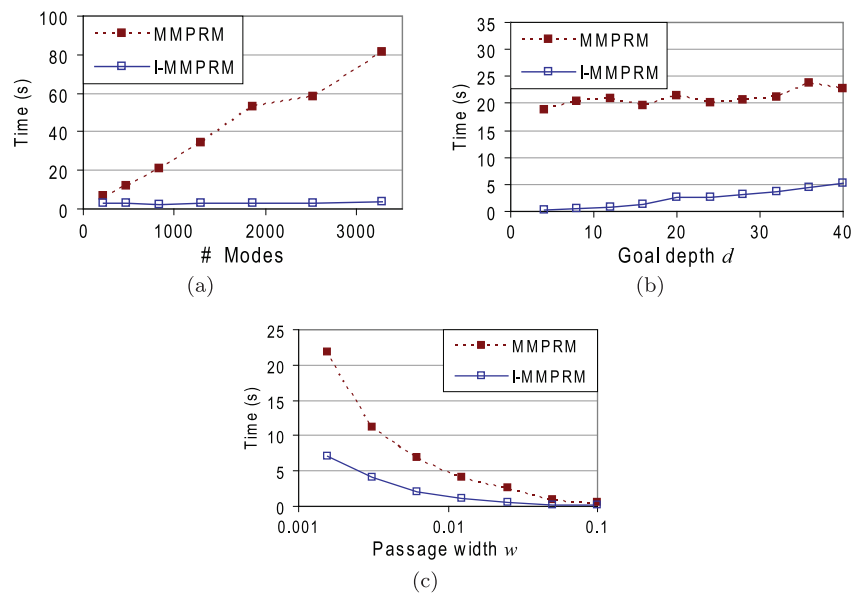


Fig. 7. Running time of Multi-Modal-PRM and Incremental-MMPRM on Example A as (a) the number of modes, (b) goal depth d , and (c) passage width w are varied independently. Results averaged over 10 runs. Here w is plotted on a logarithmic scale. The running time of MPMRM is linearly dependent the number of modes. The running time of I-MMPRM is dependent on d . Both perform better as single-mode expansiveness improves.

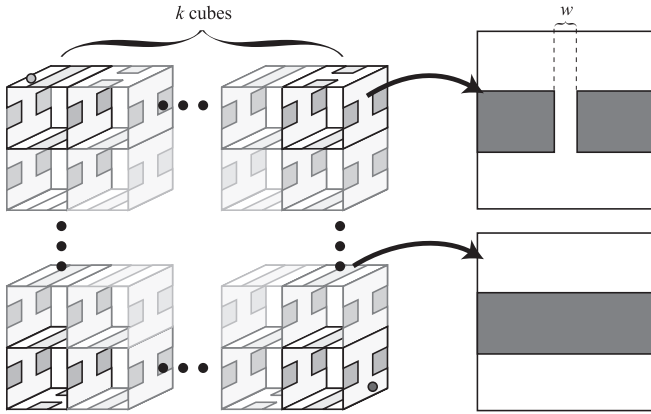


Fig. 8. In Example B, most horizontal passages are blocked, so a solution path must wind through every column of the grid. The parameter k controls the number of cubes along each side. The parameter w controls the width of the non-blocked passages.

7.2. Geometric Example B

Example B, depicted in Figure 8, is constructed such that Incremental-MMPRM performs poorly. It is similar to Example A, the difference is that we have blocked several passages such that any solution path must zig-zag along the columns in the grid, and pass through a quadratic number of modes. Furthermore, all transitions are feasible, which violates the main assumption of Incremental-MMPRM, that the existence of a transition configuration between two modes is a good indication that a feasible path connects two other configurations in those modes. We also change $N_{\text{new}} = 100$.

Figure 9 shows that Incremental-MMPRM performs no better than MMPRM. In fact, it performs worse when expansiveness is high, because it wastes time building big roadmaps which are not necessary to find a path. This will be explored further in the following section.

7.3. Sensitivity to Refinement Sample Distribution

We investigated the sensitivity of Incremental-MMPRM to the refinement sample count parameters N_{new} and N_{old} . In Examples A and B, the optimal parameters are high and low, respectively. However, these are extreme cases. In practice it is difficult to determine optimal parameters *a priori*, because their effect depends on problem characteristics, such as single-mode expansiveness and connectedness of feasible spaces, that are, in general, unobserved.

In Example A, since any candidate sequence of modes leading to the goal is guaranteed to contain a solution path, N_{new} should be large. Figure 10 plots the experimental results.

When $N_{\text{new}} = 100$ and expansiveness is low, the planner cannot find a path using only the samples allotted to the first refinement round, and many additional rounds of expansion and refinement are needed (Figure 10(b)). If N_{old} is increased to 100, fewer additional rounds are needed. If $N_{\text{new}} = 1,000$, only one round is needed.

In contrast, in Example B, Incremental-MMPRM must consider all modes as candidates to find a solution, so N_{new} and N_{old} should be small to avoid wasting samples. Figure 11 plots the experimental results. For $N_{\text{new}} = 100$, Incremental-MMPRM has approximately the same performance as Multi-Modal-PRM, and is optimal for this example. For $N_{\text{new}} = 1000$, a huge amount of time is wasted in trying to find a path in candidate mode sets where none exists.

7.4. Experiments in a Legged Locomotion Planner

In this section, we use legged locomotion as a case study to demonstrate that disconnected single-mode feasible spaces have practical implications for planning. Namely, we show that Multi-Modal-PRM is much more reliable than a prior incomplete approach that only samples one configuration in a transition. Hauser et al. (2006) gave the complete specification of the legged locomotion problem and our implementation of the planner’s subroutines (e.g. configuration sampling and constraint testing). Our experiments are performed on small restricted subsets of the legged locomotion problem, and we find that even in these subsets, disconnected feasible spaces occur often for some robots. This result runs counter to the conventional belief that disconnections are rare and can be safely ignored during planning.

Although our experiments are performed with Multi-Modal-PRM, in practice, one would solve locomotion planning problems using Incremental-MMPRM because the non-restricted mode graphs are quite large, and usually do not fit in memory.

7.4.1. Background: The Single-Trans Algorithm

In previous work we used a two-phase algorithm, here called Single-Trans. The first phase performs exploration of the mode graph (and is nearly identical to SAFT). It searches the mode graph for a sequence of footsteps to take, and a single feasible transition configuration for each step. In a second phase, single-mode paths are planned between subsequent transition configurations. If single-mode planning fails, it returns to exploration. Single-Trans solved many challenging problems for a four-limbed robot (Bretl et al. 2004) and the bipedal humanoid robot HRP-2 (Hauser et al. 2005b).

We attempted to apply Single-Trans to NASA’s ATHLETE robot (Wilcox et al. 2007), a six-legged lunar vehicle with 36 revolute joints (Figure 12). We found that even on

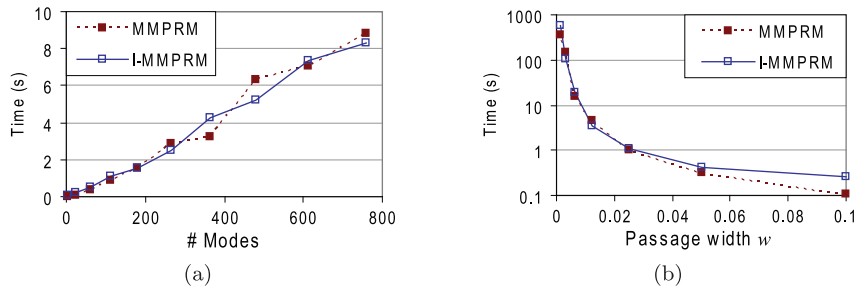


Fig. 9. Running time of Multi-Modal-PRM and Incremental-MMPRM on Example B. Results averaged over 10 runs. (a) Number of rounds as the number of modes is varied, w fixed at 0.1. (b) Number of rounds as w is varied, k fixed at 4.

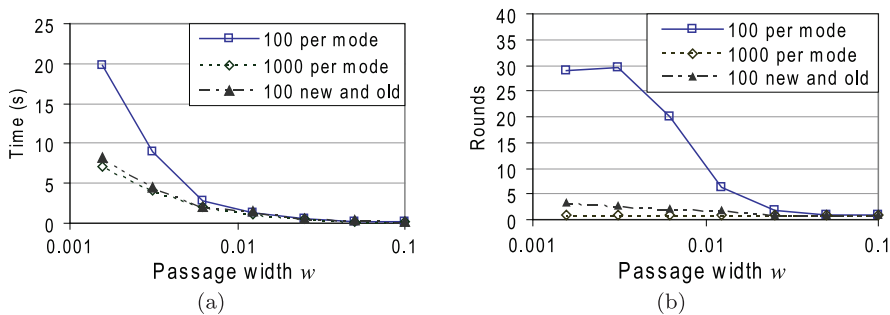


Fig. 10. Tests of Incremental-MMPRM on Example A, with different numbers of refinement samples per mode. Here k is fixed at 10. More samples result in a better running time when passage width w is low.

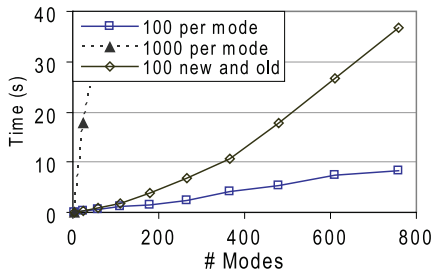


Fig. 11. Tests of Incremental-MMPRM on Example B, with different numbers of refinement samples per mode. More samples result in substantially worse running time.

seemingly simple problems, the single-mode planning phase often failed, forcing the algorithm to return often to exploration. Each exploration usually takes several minutes, leading the overall planner to have a long running time, and high variability between runs.

7.4.2. Experiments

We applied our algorithms to the ATHLETE robot and the HRP-2 robot in a variety of simulated terrains. First, we tested ATHLETE on the three test terrains of Figure 12: flat ground (Flat), a smoothly undulating terrain (Hills), and a stair step with a height of 0.5 times the diameter of ATHLETE’s chassis (Stair). We compare Single-Trans (Single Trans), Multi-Modal-PRM (MMPRM), and Multi-Modal-PRM using the connection strategy of Section 6.2 (MMPRM-C), but restrict each planner to a single sequence of modes Σ' that is known to contain a feasible path (so in essence, the mode graph is a single string of modes). In addition to allowing a comparison between algorithms, it also helps avoid variability in running time caused by the choice of footsteps. For each terrain, we computed Σ' by running Incremental-MMPRM until completion, and extracting the modes along the path. Σ' contains 34, 46, and 37 modes for Flat, Hills, and Stair, respectively.

We tested each method 10 times on identical Σ' but with different seeds to the random number generator, and terminated the planner if no path was found after 30,000 total samples. Table 1 reports the results. Single-Trans fails in

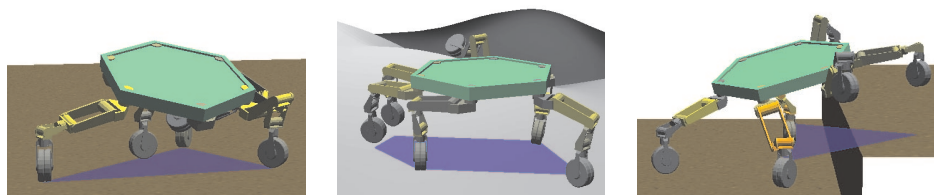


Fig. 12. Three terrains for testing the locomotion planner with ATHLETE.

Table 1. Locomotion Planning Statistics on Various Problems with a Fixed Mode Sequence, Averaged Over 10 Runs (Standard Deviations in Parentheses)

Robot	Problem	Method	Number successful	Time (s)
ATHLETE	Flat	Single Trans	0/10	501 (88.3)
		MMPRM	9/10	409 (180)
		MMPRM-C	10/10	106 (36.6)
	Hills	Single Trans	0/10	149 (29.5)
		MMPRM	10/10	181 (103)
		MMPRM-C	10/10	99.5 (28.3)
	Stair	Single Trans	0/10	258 (36.9)
		MMPRM	10/10	507 (197)
		MMPRM-C	10/10	347 (138)
HRP-2	Hills2	Single Trans	10/10	6.7 (1.0)
		MMPRM	10/10	34.5 (8.3)
		MMPRM-C	10/10	16.5 (3.4)
	Stair2	Single Trans	10/10	153.0 (160.7)
		MMPRM	10/10	438.7 (383.2)
		MMPRM-C	10/10	205.1 (123.7)
	Ladder	Single Trans	10/10	271.5 (160.8)
		MMPRM	8/10	1,543 (1,091)
		MMPRM-C	10/10	312.3 (59.1)

every case, while MMPRM and MMPRM-C successfully find a path nearly every time. They sample multiple configurations in each transition (typically around 10) before finding a solution.

Next, we performed experiments with HRP-2 on the three test terrains of Figure 13: an undulating terrain (Hills2), a 0.5 m stair step (Stair2), and a ladder with rungs 0.15 m apart (Ladder). Here Σ' contained 16, 6, and 16 modes for Hills2, Stair2, and Ladder, respectively. All three algorithms worked fairly consistently. Single-Trans is the fastest, and MMPRM-C adds some additional overhead. MMPRM took significantly longer on all three example, and timed out in a few instances. MMPRM samples “easy” and “hard” modes

evenly, so the presence of a few “hard” modes cause it to waste a lot of time.

7.4.3. Feasible Space Connectivity Evaluation

When applied to the ATHLETE robot, Single-Trans fails consistently while Multi-Modal-PRM succeeds. In this section we explicitly test the connectivity of single-mode feasible spaces, and our results support the hypothesis that Single-Trans, unfortunately, samples transition configurations in disconnected components of the feasible space, which of course cannot be connected with single-mode

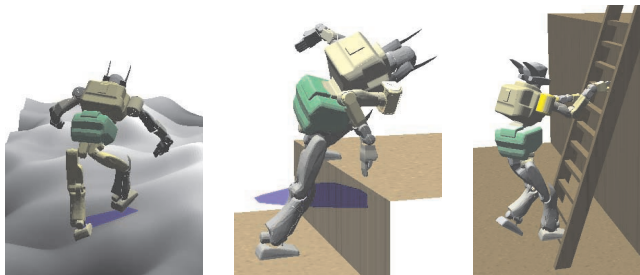


Fig. 13. Three terrains for testing the locomotion planner with HRP-2.

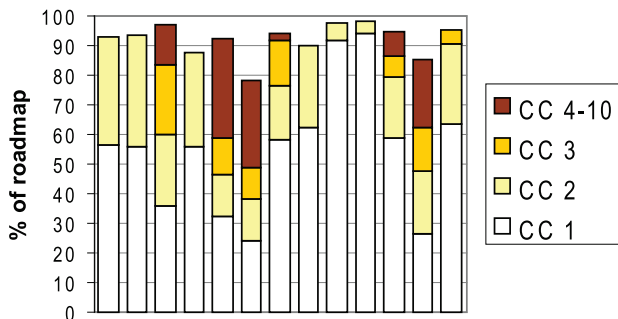


Fig. 14. Sizes of the 10 largest connected components of the disconnected modes in the Stair example.

paths. Our results also suggest that most spaces encountered by the HRP-2 robot are fully connected, which explains why *Single-Trans* works well.

For each mode σ , we build a relatively large PRM \mathcal{R}_σ by sampling 10,000 mode configurations, and 1,000 transition configurations. If less than 1,000 milestones are generated, we keep sampling until \mathcal{R}_σ contains 1,000 milestones. The large connected components in \mathcal{R}_σ are a reasonable approximation to the true connectivity of \mathcal{F}_σ . Here \mathcal{R}_σ also contains many small, spurious components, which usually become aggregated into larger components when more samples are added. Thus, we do not count any components from \mathcal{R}_σ that contain less than 1% of total milestones.

The results on the ATHLETE examples as follows. Of the modes in Σ' for the Flat, Hills, and Stair examples, 7/34, 9/46, and 13/37 modes, respectively, have multiple connected components. Of those, more than half have three or more components. Figure 14 plots the component sizes for each disconnected mode for the Stair example. We also computed that the probability that *Single-Trans* samples transition configurations in the same connected component of \mathcal{F} is approximately 0.18%, 0.35%, and 0.12%. Repeating these tests on the HRP-2 examples, we found that each mode contains a single component.

Upon further inspection, we found that each pair of components can usually be separated in a single joint—that is, there exists a joint k and a value θ such that all configurations q in one component have $q_k < \theta$ and those in the other component have $q_k > \theta$, where q_k is the k th joint angle of q . The joint is typically one of the two joints closest to the ground in a support leg. At this stage we do not have a clear explanation as to why this is the case. Future work could eliminate disconnections by using the planner to help developing better robot designs or footfall selection criteria.

8. Conclusion

In this paper we have presented *Multi-Modal-PRM*, a new sample-based multi-modal planning algorithm for problems with a finite number of modes. We have proved that *Multi-Modal-PRM* has probability of failure exponentially converging to 0 in the number of samples drawn, if the feasible space of each mode is expansive relative to its embedded submanifold. We have also presented a variant, *Incremental-MMPRM*, which restricts planning to an incrementally growing set of candidate modes. *Incremental-MMPRM* is orders of magnitude faster than *Multi-Modal-PRM* in problems with large numbers of modes. We have demonstrated the reliability of these techniques in experiments in a locomotion planner.

When applied to the ATHLETE six-legged robot, *Multi-Modal-PRM* dramatically improves the planner’s reliability over a simpler incomplete method. When applied to a humanoid biped, *Multi-Modal-PRM* modestly improves reliability with moderate overhead. We evaluate the hypothesis that *Multi-Modal-PRM* improves reliability by properly handling multiple connected components in single-mode feasible spaces. Indeed, our experiments suggest that disconnected feasible spaces occur frequently in ATHLETE, and rarely occur in the biped. A promising avenue for future work is to use feasible space connectedness as a robot design criterion.

The completeness results in this paper hold only when the number of modes is finite. However, many problems have a continuous (uncountably infinite) number of modes. For example, the footfalls of a legged robot could be anywhere on a given two-dimensional surface. In this case, we can discretize the continuous mode set by sampling a finite number of foot placements (possibly with a bias toward “promising” placements). Then, the completeness results in this paper hold only if the selected finite subset of modes contains a solution path. If no such path exists, the modes may have been selected poorly. Future research should investigate the completeness and convergence rate of multi-modal planners that sample modes from continuous sets of modes (e.g. Hauser et al. (2007), Sahbani et al. (2002), and van den Berg et al. (2008)).

Appendix: Probabilistic Roadmaps and Expansiveness

In this appendix we review the basic PRM algorithm and its theoretical completeness properties in expansive spaces.

A.1. Basic PRM Algorithm

PRM planners address the problem of connecting two configurations q_{start} and q_{goal} in the feasible space \mathcal{F} , a subset of configuration space \mathcal{C} . While it is prohibitively expensive to compute an exact representation of \mathcal{F} , feasibility tests for individual configurations are usually very cheap. So to approximate the connectivity of \mathcal{F} , PRM planners build a *roadmap* \mathcal{R} , a network of sampled feasible configurations (called *milestones*) connected with straight-line segments. In the basic PRM algorithm, milestones are obtained by sampling \mathcal{C} uniformly at random and rejecting the configurations sampled outside \mathcal{F} . More sophisticated PRM algorithms use non-uniform probabilistic measures to sample \mathcal{C} . They are usually more efficient than the basic algorithm, but they are also much more difficult to analyze formally and the gains in efficiency are usually measured empirically through experiments.

The basic PRM algorithm is given in Algorithm 3.

Algorithm 3 BASIC-PRM($q_{\text{start}}, q_{\text{goal}}, n$)

Initialize the roadmap \mathcal{R} with q_{start} and q_{goal} as only two milestones.

Repeat n times:

1. Sample a configuration q uniformly from \mathcal{C} and test its feasibility. Repeat until a feasible sample is found.
2. Add q to \mathcal{R} as a new milestone. Connect it to milestones q' in \mathcal{R} if the line segment between q and q' lies in \mathcal{F} .

If \mathcal{R} contains a path between q_{start} and q_{goal} , return this path. Otherwise, return “failure”.

If a PRM planner produces a path successfully, the path is guaranteed to be feasible, but if it fails, then we cannot tell whether no path exists or the cutoff n on the number of milestones was set too low.

A.2. Performance in Expansive Spaces

BASIC-PRM and several variants have been shown to be probabilistically complete, that is, the probability of incorrectly returning failure approaches 0 as n increases. One particularly strong completeness theorem proves that PRMs converge exponentially when \mathcal{F} is *expansive* (Hsu et al. 1997, 1999).

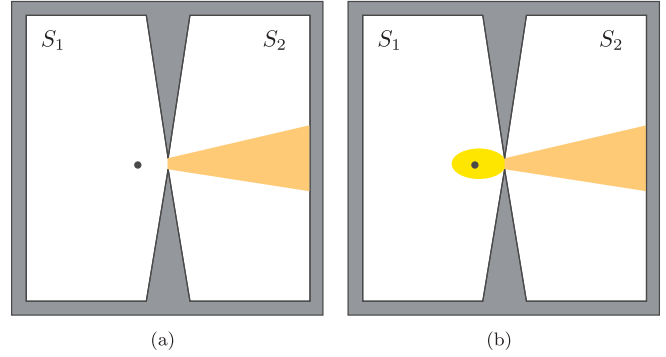


Fig. 15. A poorly expansive space. (a) The visibility set $\mathcal{V}(q)$ in region S_2 , of a point q in S_1 . (b) $\text{LOOKOUT}_\beta(S_1)$ is the set of points that see at least a β fraction of S_2 .

The notion of expansiveness expresses the difficulty of constructing a roadmap that captures the connectivity of \mathcal{F} . The success of PRM planners in high-dimensional spaces is partially explained by the fact that expansiveness is not explicitly dependent on the dimensionality of \mathcal{F} . Let $\mu(S)$ measure the volume of any subset $S \subseteq \mathcal{F}$ (with $\mu(\mathcal{F})$ finite and normalized to 1), and let $\mathcal{V}(q)$ be the set of all points that can “see” q in \mathcal{F} , i.e. that can be connected to q with a straight line in \mathcal{F} . The *lookout* set of a subset S of \mathcal{F} is defined as the subset of S that can see a substantial portion of the complement of S (see Figure 15). Formally, given a constant $\beta \in (0, 1]$ and a subset S of a connected component \mathcal{F}' in \mathcal{F} , define

$$\text{LOOKOUT}_\beta(S) = \{q \in S \mid \mu(\mathcal{V}(q) \setminus S) \geq \beta \mu(\mathcal{F}' \setminus S)\}.$$

For constants $\epsilon, \alpha, \beta \in (0, 1]$, \mathcal{F} is said to be $(\epsilon, \alpha, \beta)$ -*expansive* if:

1. For all $q \in \mathcal{F}$, $\mu(\mathcal{V}(q)) \geq \epsilon \mu(\mathcal{F})$.
2. For any connected subset S , $\mu(\text{LOOKOUT}_\beta(S)) \geq \alpha \mu(S)$.

The first property, known as ϵ -goodness (Kavraki et al. 1998), states that each configuration sees a significant fraction of \mathcal{F} . Note that it implies that the volume of each connected component of \mathcal{F} is at least ϵ . This observation is used in the proof of Lemma 3 in Section 4.4.

The second property can be roughly interpreted as stating that if a connected component of \mathcal{F} is partitioned into (S, \bar{S}) , then a significant portion of S can see a significant portion of \bar{S} . Its significance is as follows. View S as the visibility set of a single roadmap component \mathcal{R}' , i.e. the subset of configurations in \mathcal{F} that are seen by at least one milestone of \mathcal{R}' . Let \mathcal{F}' be the connected component of \mathcal{F} in which S lies. Then, with significant probability (at least $\alpha \mu(S)$), a configuration picked uniformly at random from \mathcal{F} will simultaneously connect to \mathcal{R}' and significantly reduce the fraction of \mathcal{F}' not visible to \mathcal{R}' (by at least β).

The primary convergence result of Hsu et al. (1997, 1999) can be restated as follows.

Theorem 2. *If \mathcal{F} is $(\epsilon, \alpha, \beta)$ -expansive, then the probability that a roadmap of n uniformly, independently sampled milestones fails to connect q_{start} and q_{goal} is no more than ce^{-dn} for some positive constants c and d .*

The constants c and d are elementary functions of ϵ , α , and β . In particular,

$$c = \frac{8}{\epsilon\alpha} \exp\left(\frac{\epsilon\alpha}{8} + \frac{3\epsilon\alpha}{8\beta}\right) \quad (8)$$

and

$$d = \frac{\epsilon\alpha}{16}. \quad (9)$$

If \mathcal{F} is favorably expansive (ϵ , α , and β are high), the bound decreases to zero quickly, and BASIC-PRM will find a path between q_{start} and q_{goal} relatively quickly. If, on the other hand, \mathcal{F} is poorly expansive (ϵ , α , and β are low), then PRM performance might be poor for certain query configurations q_{start} and q_{goal} . A complementary theorem proven by Hsu et al. (2006) states that a PRM planner will succeed with arbitrarily low probability for any fixed n in spaces with small α and β .

References

- Akinc, M., Bekris, K. E., Chen, B. Y., Ladd, A. M., Plaku, E. and Kavraki, L. E. (2003). Probabilistic roadmaps of trees for parallel computation of multiple query roadmaps. *International Symposium on Robotics Research*, Siena, Italy.
- Alami, R., Laumond, J.-P. and Siméon, T. (1995). Two manipulation planning algorithms. *Algorithmic Foundations of Robotics*, Goldberg, K., Halperin, D., Latombe, J.-C. and Wilson, R. (eds). Wellesley, MA, A K Peters, pp. 109–125.
- Boor, V., Overmars, M. and van der Stappen, A. (1999). The Gaussian sampling strategy for probabilistic roadmap planners. *International Conference on Robotics and Automation*, pp. 1018–1023.
- Bretl, T., Lall, S., Latombe, J.-C. and Rock, S. (2004). Multi-step motion planning for free-climbing robots. *Workshop on the Algorithmic Foundations of Robotics*, Zeist, the Netherlands.
- Chaudhuri, S. and Koltun, V. (2007). Smoothed analysis of probabilistic roadmaps. *Fourth SIAM Conference of Analytic Algorithms and Computational Geometry*.
- Choset, H., Lynch, K., Hutchinson, S., Kantor, G., Burgard, W., Kavraki, L. and Thrun, S. (2005). *Principles of Robot Motion: Theory, Algorithms, and Implementations*. Cambridge, MA, MIT Press.
- Cortés, J. and Siméon, T. (2004). Sampling-based motion planning under kinematic loop-closure constraints. *Workshop on the Algorithmic Foundations of Robotics*, Zeist, the Netherlands.
- Hauser, K., Bretl, T. and Latombe, J.-C. (2005a). Learning-assisted multi-step planning. *IEEE International Conference on Robotics and Automation*, Barcelona, Spain.
- Hauser, K., Bretl, T. and Latombe, J.-C. (2005b). Non-gaited humanoid locomotion planning. *IEEE International Conference on Humanoid Robots*, Tsukuba, Japan.
- Hauser, K., Bretl, T., Latombe, J.-C., Harada, K. and Wilcox, B. (2006). Motion planning for legged robots on varied terrain. *The International Journal of Robotics Research*, **27**(11–12): 1325–1349.
- Hauser, K., Ng-Thow-Hing, V. and Nos, H. G.-B. (2007). Multi-modal planning for a humanoid manipulation task. *International Symposium on Robotics Research*, Hiroshima, Japan.
- Hoeffding, W. (1996). Probability inequalities for sums of bounded random variables. *Journal of the American Statistical Association*, **58**(301): 13–30.
- Hsu, D., Kavraki, L. E., Latombe, J.-C., Motwani, R. and Sorkin, S. (1998). On finding narrow passages with probabilistic roadmap planners. *Workshop on the Algorithmic Foundations of Robotics*, Natick, MA, pp. 141–153.
- Hsu, D., Kindel, R., Latombe, J.-C. and Rock, S. (Mar 2002). Kinodynamic motion planning amidst moving obstacles. *The International Journal of Robotics Research*, **21**(3): 233–255.
- Hsu, D., Latombe, J. and Kurniawati, H. (2006). On the probabilistic foundations of probabilistic roadmap planning. *The International Journal Robotics Research*, **25**(7): 627–643.
- Hsu, D., Latombe, J.-C. and Motwani, R. (1997). Path planning in expansive configuration spaces. *IEEE International Conference on Robotics and Automation*, pp. 2219–2226.
- Hsu, D., Latombe, J.-C. and Motwani, R. (1999). Path planning in expansive spaces. *The International Journal of Computational Geometry and Applications*, **9**(4–5): 495–512.
- Kavraki, L., Latombe, J., Motwani, R. and Raghavan, P. (1998). Randomized query processing in robot motion planning. *Journal of Computer and System Sciences*, **57**(1): 50–60.
- Kavraki, L., Svetstka, P., Latombe, J. and Overmars, M. (1996). Probabilistic roadmaps for path planning in high-dimensional configuration spaces. *IEEE Transactions on Robotics and Automation*, **12**(4): 566–580.
- Koga, Y. and Latombe, J.-C. (1994). On multi-arm manipulation planning. *IEEE International Conference on Robotics and Automation*, San Diego, CA, pp. 945–952.
- LaValle, S. M. and Kuffner, Jr, J. J. (2001). Randomized kinodynamic planning. *The International Journal of Robotics Research*, **20**(5): 379–400.
- LaValle, S. M., Yakey, J. H. and Kavraki, L. E. (1999). A probabilistic roadmap approach for systems with closed kinematic chains. *IEEE International Conference on Robotics and Automation*, Detroit, MI.

- Nielsen, C. L. and Kavraki, L. E. (2000). A two level fuzzy PRM for manipulation planning. *IEEE/RSJ International Conference on Intelligent Robots and Systems*, pp. 1716–1721.
- Nieuwenhuisen, D., van der Stappen, A. F. and Overmars, M. H. (2006). An effective framework for path planning amidst movable obstacles. *Workshop on the Algorithmic Foundations of Robotics*, New York, NY.
- Sahbani, A., Cortés, J. and Siméon, T. (2002). A probabilistic algorithm for manipulation planning under continuous grasps and placements. *IEEE/RSJ International Conference on Intelligent Robots and Systems*, Lausanne, Switzerland, pp. 1560–1565.
- Sánchez, G. and Latombe, J.-C. (2002). On delaying collision checking in PRM planning: Application to multi-robot coordination. *The International Journal of Robotics Research*, **21**(1): 5–26.
- Stilman, M. (2007). *Navigation Among Movable Obstacles*. PhD thesis, Carnegie Mellon University.
- van den Berg, J., Stilman, M., Kuffner, J., Lin, M. and Manocha, D. (2008). Path planning among movable obstacles: A probabilistically complete approach. *Workshop on the Algorithmic Foundations of Robotics*.
- Wilcox, B. H., Litwin, T., Biesiadecki, J., Matthews, J., Heverly, M., Morrison, J., Townsend, J., Ahmad, N., Sirota, A. and Cooper, B. (2007). Athlete: A cargo handling and manipulation robot for the Moon. *Journal of Field Robotics*, **24**(5): 421–434.